

Suitability Evaluation of Land Use/ Land Cover (LULC) Towards Landslide Prone Areas in Structural and Volcano Landform

Arrasyid, R.,^{1*} Ihsan, H. M.,² Darsiharjo² Ruhimat, M.² and Pratama, A. R.³

¹Tourism Education, Faculty of Social Sciences Education, Universitas Pendidikan Indonesia, Indonesia
E-mail: rikoarraysid@upi.edu

²Geography Information Science, Faculty of Social Sciences Education, Universitas Pendidikan Indonesia
Indonesia, E-mail: haikalmihsan@upi.edu, darsiharjo@upi.edu, mamatruhimat@upi.edu

³Manajemen Resort Leisure, Faculty of Social Sciences Education, Universitas Pendidikan Indonesia
Indonesia, E-mail: armandharedo@upi.edu

*Corresponding Author

DOI: <https://doi.org/10.52939/ijg.v19i6.2697>

Abstract

North Bandung area covering structural landforms and volcanoes has an active volcano and fault, leading to potential of landslide. This study aims to create a new scheme of LULC zones based on a landslide prone area. The landslide zone is analyzed through Fuzzy through the following variables: rainfall, drainage distance, drainage density, slope angle, slope aspect, distance lineament, elevation, slope curvature, and topographic wetness index (TWI). The LULC is created based on Landsat-8 image. The suitability evaluation of the LULC area is analyzed using overlay union and query to obtain region suitability results. The landslide analysis results in three classifications including high (3.626,97 ha), medium (5.294,53 ha), and low (1.117,69 ha). It is also found that there is a functional change by 11.87% (4,632.01 ha) from the total area as well as a type change from rice field and built-up into orchard and field. On the functional shift classification of orchard, the land can be used for palms, bamboo, kawung, and sugar palm whose core has small roots gripping the ground material enabling them to have high vegetation density. On the land with 15% slope, terracing and annual planting are recommended to keep the land productive and reduce landslide prone.

Keywords: Landslide, Land Use/Land Cover, Structural Landform, Volcano Landform

1. Introduction

Structural landforms and volcanoes commonly have high topography and steep slope causing the area to be landslide prone. The danger of landslide commonly occur in hilly areas [1], such as structural landforms and volcanoes in North Bandung, Indonesia. In mountainous areas, landslide is considered the primary mass wasting process [2]. Usually there are rocks and weathered materials prone to fall in the direction of gravity in the structural landforms and volcanoes leading to landslide [3]. In addition, meteorological and hydrological aspects can also by indicators of landslide [4]. Landslide hazard mapping technology has been widely developed. Landslides occur according to the characteristics of the area in general, but it can be estimated which areas have the highest potential for hazard [5]. Geographic Information System (GIS) technology is able to map landslide hazards with landslide triggering parameters and the

environment [6]. In GIS modeling, landslides can be mapped using fuzzy statistics [7] and overlay statistics [8]. Remote sensing (RS) technology can be an excellent alternative in assessing landslide parameters related to geographical aspects of the earth's surface or terrain [9].

The terrain aspect of the earth's surface is certainly a parameter that can determine the potential for landslide hazard. Steep slopes are an indication of landslide hazard [10]. Aspect is a slope face which influences slope stability [11]. Curvature is the shape of the slope that influences the occurrence of landslides [11]. Drainage parameters that affect runoff and erosion triggers are drainage distance [12] and drainage density [13]. TWI is an indication of soil material moisture which represents soil erosion [14]. In the area near the structure is a weak zone where weathered material and open pores make the soil easy to erode [12].

Rain is a meteorological aspect that triggers erosion [15] on a volcanic structural landform. Land-use/land-cover (LULC) is the part of the earth's surface that will affect landslide events [16]. Areas with development types, deforestation, expansion of agricultural land are areas prone to landslides [17]. Human activity by changing land use is an indicator of changes in slope stability in mountainous areas [18]. Remote Sensing (RS) technology is able to assess LULC conditions with freely available satellite imagery [19]. Landslides have a considerable impact on socio-economic aspects both at the local and national levels [12]. The LULC area must be adapted to the surrounding disaster conditions such as landslides, in order to reduce risks in disaster-prone areas, so that the development of an area is sustainable.

The North Bandung area is part of the volcanic landform area and structural faults. This area contains an active volcano, namely Mount Tangkuban Parahu, and an active fault, namely the Lembang Fault. In this area there are many built-up areas that are established in landslide-prone areas, besides that there are also LULCs that are vulnerable if built in landslide-prone areas. The purpose of this

study is to create a new scheme for LULC zones based towards landslide hazard conditions in Structural and Volcano landforms. This mapping scheme will be very useful for local governments in planning development. This research has not been done much, usually LULC as a parameter triggering landslides, while here is making a landslide-based LULC mapping suitability scheme.

2. Study Area

This research was conducted in the North Bandung Region, Indonesia with an area of 389,598 km². The North Bandung area has an altitude between 728 MSL – 2202 MSL. Based on the Geological Map Sheet of Bandung, Java, it was found that the North Bandung area is a structural and volcanic area. In this area there is a fault known as the Lembang fault. This fault is an active fault that stretches from west to east. In the north there is an active volcano, namely Mount Tangkuban Parahu. This condition makes the North Bandung Area vulnerable to landslides as a result of endogenous and exogenous forces, so that a LULC suitability study for landslides is very suitable to be carried out in this area (Figure 1).

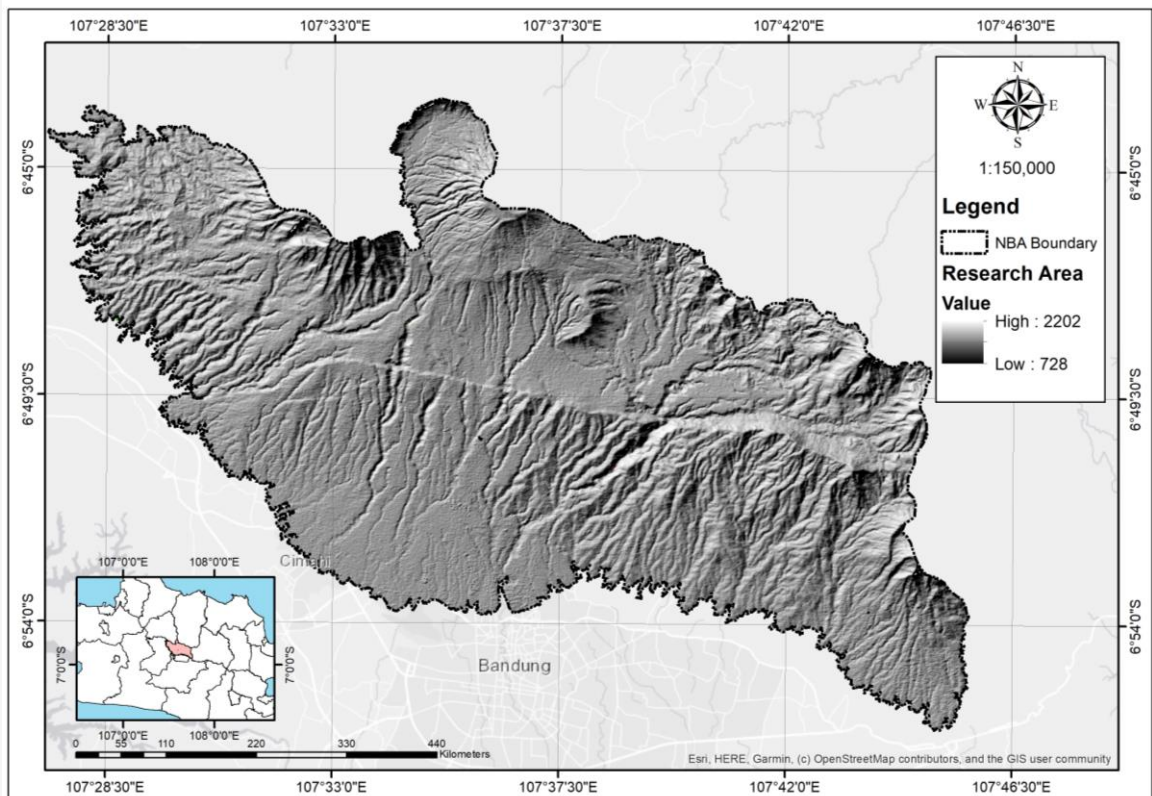


Figure 1: Research area, North Bandung area map

3. Data and Method

3.1 Rainfall

The heavier the rain, the more potential emerges. Rain will trigger landslides if it falls on areas of unsaturated soil and then has steep slopes [15]. High rain intensity in mountainous areas can trigger slope stability, water will experience runoff or infiltration, certain materials will trigger landslides [20]. Rain is studied using the Inverse Weighting Model (IDW) method at each rain post point using GIS software. Rainfall data is visualized spatially using interpolation methods such as IDW [21]. The IDW used uses the following formula:

$$P_i = \frac{\sum_{x=1}^n \left(\frac{1}{dx^t} \times P_x \right)}{\sum_{x=1}^n \frac{1}{dx^t}}$$

Equation 1

Equation explains that P_i is the prediction of rainfall at a location adjusted for location i . P_x is the representative of rainfall in the neighboring location x , while dx is the distance from location x to location i which is predicted for rainfall. The equation also explains that n is the number of neighbors t which is a positive real number and the power function value was used in the interpolation [21]. The IDW technique has been carried out in GIS software.

3.2 Drainage Distance

The closer the more potential, because it affects the stability of the slope. Distance to river. The distance of the river indicates slope stability in lateral stress relief, usually 100m [12], river flow will wet or erode the bottom of the slope so that it becomes part of the erosion process. This section will be analyzed using a buffer with a distance of 50m for each session, and contains 3 sessions. Drainage will be extracted from DEMNAS and the analysis buffer will be processed using GIS software.

3.3 Drainage Density

The denser it is, the more potential it has, because it is related to water runoff, the denser it is, the more runoff and the more the surface is eroded so that there is a possibility of erosion [22]. Low density values indicate permeable subsurface material, low relief terrain and dense vegetation, so there is no potential for landslides [13]. Drainage density will be assessed using GIS software. Drainage will be extracted from DEMNAS and drainage density will be processed through GIS software.

3.4 Slope Angle

The steeper it is, the more vulnerable it is, because the gravity is higher [23]. Slope angle is an important parameter in the study of slope stability. In this study, the slope will be extracted through DEMNAS and analyzed using GIS software. The steep slope area indicates the occurrence of high runoff in areas with low vegetation cover, so the potential for erosion is high. Rain conditions with steep slopes and unsaturated material can trigger slope stability [24]. The slope angle will be processed using GIS software.

3.5 Slope Aspect

Slope aspects are very important factors that affect the natural environment around the slopes such as solar radiation, vegetation cover and soil moisture, and the mass of soil and rock around the slope surface can gradually deteriorate under some negative conditions [25]. The slope aspect greatly influences hydrological processes through evapo-transpiration and thus affects weathering processes and vegetation and root development [26]. Aspect also affects soil moisture and vegetation cover so that it becomes the initiation of landslides. The slope aspect affects hydrological phenomena, evapotranspiration, regulating soil moisture, vegetation and grass, and root penetration. This shows or results in differences in soil moisture and vegetation area in terms of the direction of sunlight, and plays a considerable role in the distribution of discontinuities and the occurrence of landslides. Therefore, the slope aspect has an indirect relationship with the occurrence of landslides and their level of vulnerability [27].

3.6 Distance Lineament

The closer to the lineament the more potential it is, because the zone (faulted, fractured, folded) is a relatively broken unit such as oscillating [12]. This condition makes the slope unstable so that there are landslides. The lineament zone is a weak zone, because it is part of the fluid circulation which weathers the material and opens pores so that water can easily enter [12]. Lineaments were extracted through DEMNAS and distance lineaments were analyzed using GIS software. In this study, the distance lineament will be analyzed using a buffer with a distance of 50m, each session containing 3 sessions. The lineament will be extracted from DEMNAS and the analysis buffer will be processed using GIS software.

3.7 Elevation

The higher an area, the more potential for landslides, because it will be related to the material and slope [10]. Elevation can be analyzed using DEM through GIS software [28]. DEMNAS is a DEM product that will be used in elevation studies. The assumption is that areas with high elevations are related to slope, aspect, curvature, water runoff and material type. This condition will certainly affect the stability of the slope.

3.8 Slope Curvature

Curvature will affect slope stability, because it reflects the shape of slopes such as concave, convex and straight [17]. Conventionally, convex slopes have a positive curvature value, while concave slopes have a negative curvature value. In addition, slopes with a curvature value of 0 have straight and smooth surfaces [11]. Curvature is an indication of slope stability. Curvature is extracted through DEMNAS and processed using GIS software.

3.9 TWI (Topographic Wetness Index)

The higher the TWI value, the greater the potential for landslides, because landslides are unlikely to occur on stable flat land [14]. TWI is a representation of soil moisture and water accumulation, so it has indications for landslide studies [29]. TWI can measure topographic control in areas of water saturation patterns in hydrological processes [30]. TWI studies can be processed through SAGA GIS using DEMNAS [31].

3.10 Land Use Land Cover (LULC)

The LULC type will affect geographical and environmental conditions in controlling soil surface degradation [17]. Understanding the relationship between LULC and landslide events is important to study for risk management [32]. LULC will be analyzed extracted from Landsat 8 OLI (Operational Land Imager) in 2022 using remote sensing software. LULCs with low dense vegetation have the potential for landslides, whereas those in open areas or built-up areas have a high potential for landslides [33]. The analysis used for the LULC study is Supervised classification with the LULC type, namely thickets/shrubs, forests, gardens, fields/moors, settlements, grass, paddy fields, rocky areas and bodies of water.

3.11 Fuzzy Analysis of Landslide

Landslide hazard maps are made using fuzzy analysis in ArcGIS software. Each parameter is a raster data that has a pixel value. The pixel value will be changed to the lowest 0 and the highest 1, using fuzzy

membership tools. Each parameter will be overlaid using fuzzy analysis according to the specified score. Fuzzy analysis is a tool in GIS software that can be used for spatial statistics, using several parameters according to the study. There is a tool called Fuzzy Membership in ArcGIS Software that can process the analysis. The type of fuzzy membership used was the linear type. Specifies the algorithm used in fuzzification of the input raster. Certain settings for Membership type employ a Spread parameter to determine how rapidly the fuzzy membership values decrease from 1 to 0. Calculates membership based on the linear transformation of the input raster. Assigns a membership value of 0 at the minimum and a membership of 1 at the maximum. Fuzzy membership is determined by adjusting the application function, where the range of values is 0-1, so it is divided into three range values between 0-1, namely 0.333, 0.666 and 1.

The fuzzy value is determined by the fuzzy membership algorithm on ArcGIS tools. Fuzzy weight is determined from fuzzy overlay analysis. Fuzzy membership describes the classification of each parameter, while the fuzzy weight is the parameter value for overlay analysis. After that, each parameter has a value that is ready to be overlaid using fuzzy analysis in ArcGIS. In this study, 3 classifications will be made, namely Low, Medium and High. The overlay type for fuzzy is and with a gamma value of 0.9. First, use the Reclassify tool to provide a new range of values (for example, 1 to 100). Divide the result by a factor (for example, by 100) to normalize the output values to be between 0.0 and 1.0. Certain settings for Membership type employ a Spread parameter to determine how rapidly the fuzzy membership values decrease from 1 to 0. Linear—Calculates membership based on the linear transformation of the input raster. Assigns a membership value of 0 at the minimum and a membership of 1 at the maximum. For the Linear membership function, the input raster must be ordered data. The minimum can be less than the maximum to create a positive slope or greater than the maximum to create a negative slope for the transformation. If the minimum is less than the maximum, a positive-sloped function is used for the transformation; if the minimum is less than the maximum, a negative-sloped function is used.

3.12 LULC Recommendation

The results of the landslide hazard map will be overlaid intersect on GIS software with LULC to get overlapping results between landslide prone areas and land use types. Area suitability will be focused on high landslide-prone areas.

The intersect technique will provide spatial information on separate data variables into a single unit. The LULC criteria that are vulnerable to landslide hazard are built-up areas, so if there is a built-up area in the high zone, it will be recommended to change land use. Other areas such as plantations and fields/moor fields. In this area, of course, it can be engineered, such as making swales or planting landslide support plants. The visualized LULC areas are thickets/shrubs, forests, gardens, fields/moor fields, settlements, grass, paddy fields, rocky areas and bodies of water.

4. Result

4.1 Rainfall

Rainfall in the study area is susceptible to 1983.81 mm/year to 1764.18 mm/year. There are 3 rain posts

used in the rain calculation, namely Ambon wood with an average rainfall of 1983.81 mm. year, lembang 1894 mm/year and dago expert 1764.18 mm/year. The highest rainfall is in the combined area of the Lembang fault line and the Tangkuban Parahu volcano area, while the lowest rainfall is spread in the southern area of the study which is part of the lowest plains. Rain in the study area on average is orographic rain, because the rain falls in mountainous areas. In the western and eastern parts it has relatively almost the same scattered rain pattern, this condition is caused by the situation of the monsoon winds blowing according to the season, so the rain characteristics are almost the same. This condition is illustrated in the visualization of Figure 2.

Table 1: Research parameter

No	Type	Fuzzy Membership Value	Information	Classification
1	Rainfall	0.333	1830.72 mm	Low
		0.666	1897.27 mm	Medium
		1.000	1963.81 mm	High
2	Distance drainage	0.333	100 m	Low
		0.666	200 m	Medium
		1.000	300 m	High
3	Drainage density	0.333	3.85 km ²	Low
		0.666	7.70 km ²	Medium
		1.000	11.56 km ²	High
4	Slope angle	0.333	Flatt undulating	Low
		0.666	Moderately sloping Hilly	Medium
		1.000	Steep Very steep	High
5	Slope aspect	0.333	Flat North Northeast	Low
		0.666	East Southeast South	Medium
		1.000	Southwest West Northwest	High
6	Distance Lineament	0.333	100m	Low
		0.666	200m	Medium
		1.000	300m	High
7	Elevation	0.333	1219.33 MSL	Low
		0.666	1710.667 MSL	Medium
		1.000	2202 MSL	High
8	Curvature	0.333	Convex	Low
		0.666	Flat	Medium
		1.000	Concave	High
9	TWI	0.333	8.86 km ²	Low
		0.666	16.49 km ²	Medium
		1.000	24.13 km ²	High

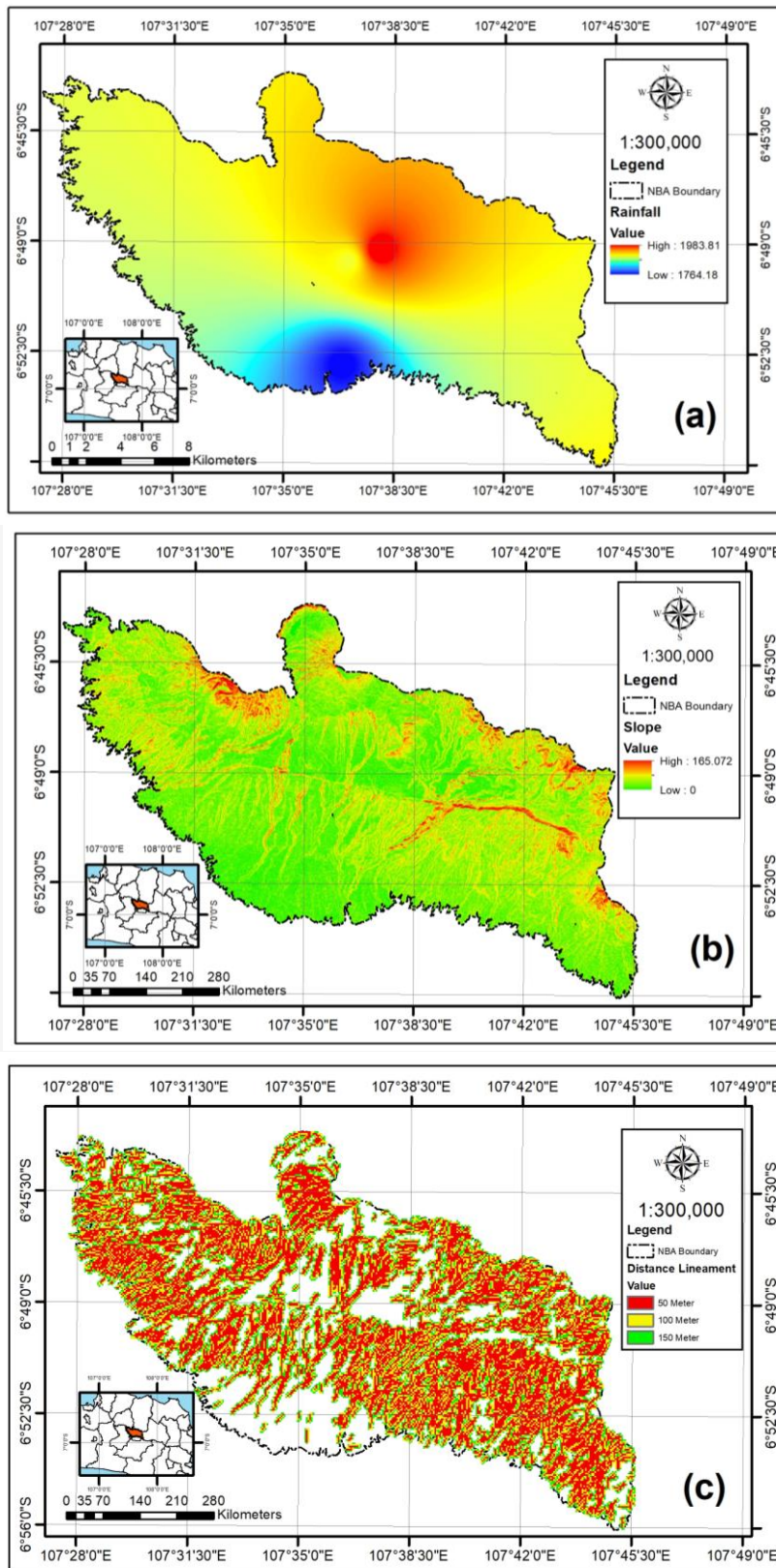


Figure 2: Variable landslide (a) Rainfall, (b) Slope, (c) Lineament distance

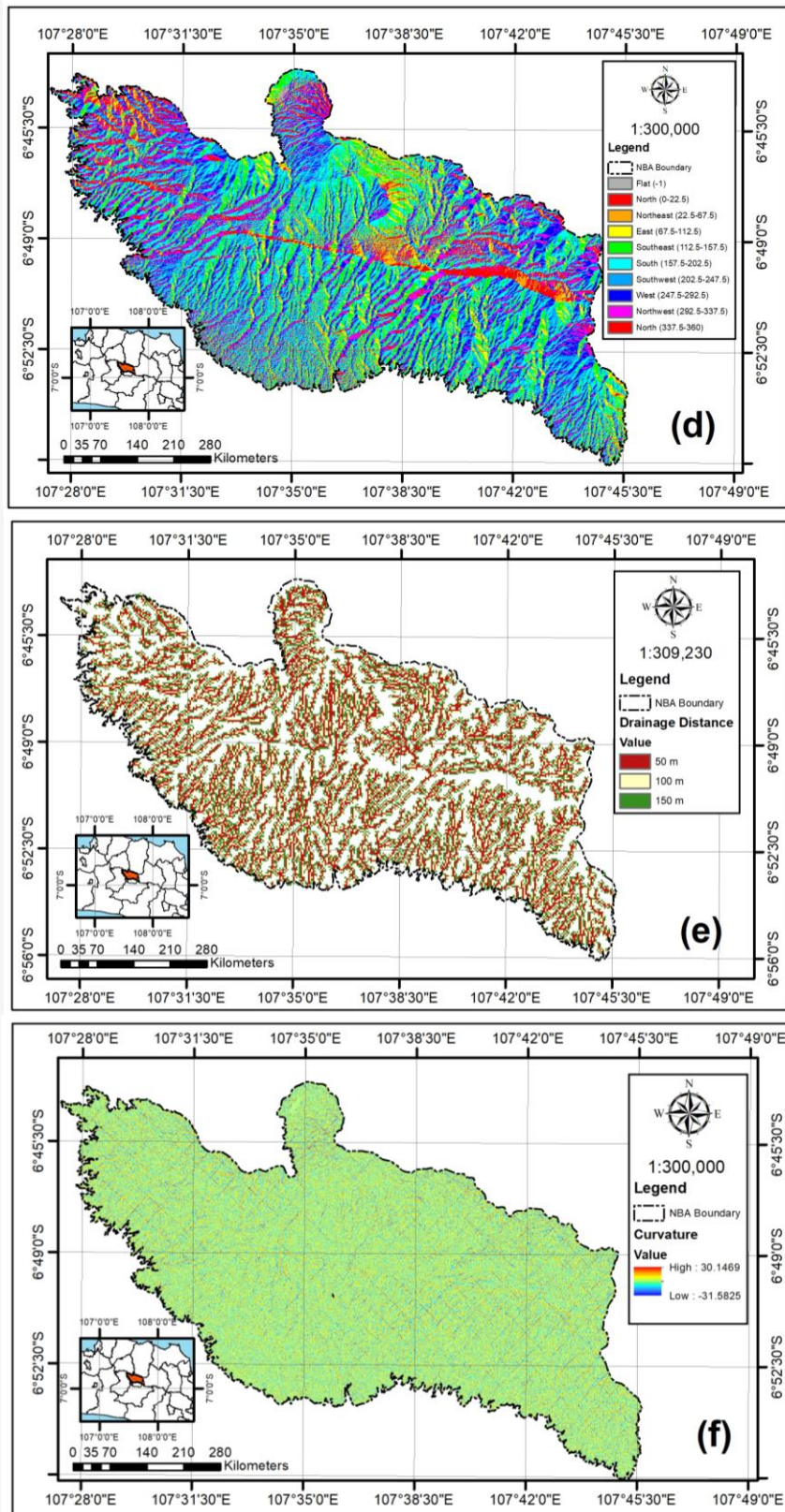


Figure 2: Variable landslide (d) Slope aspect, (e) Drainage distance, (f) Curvature

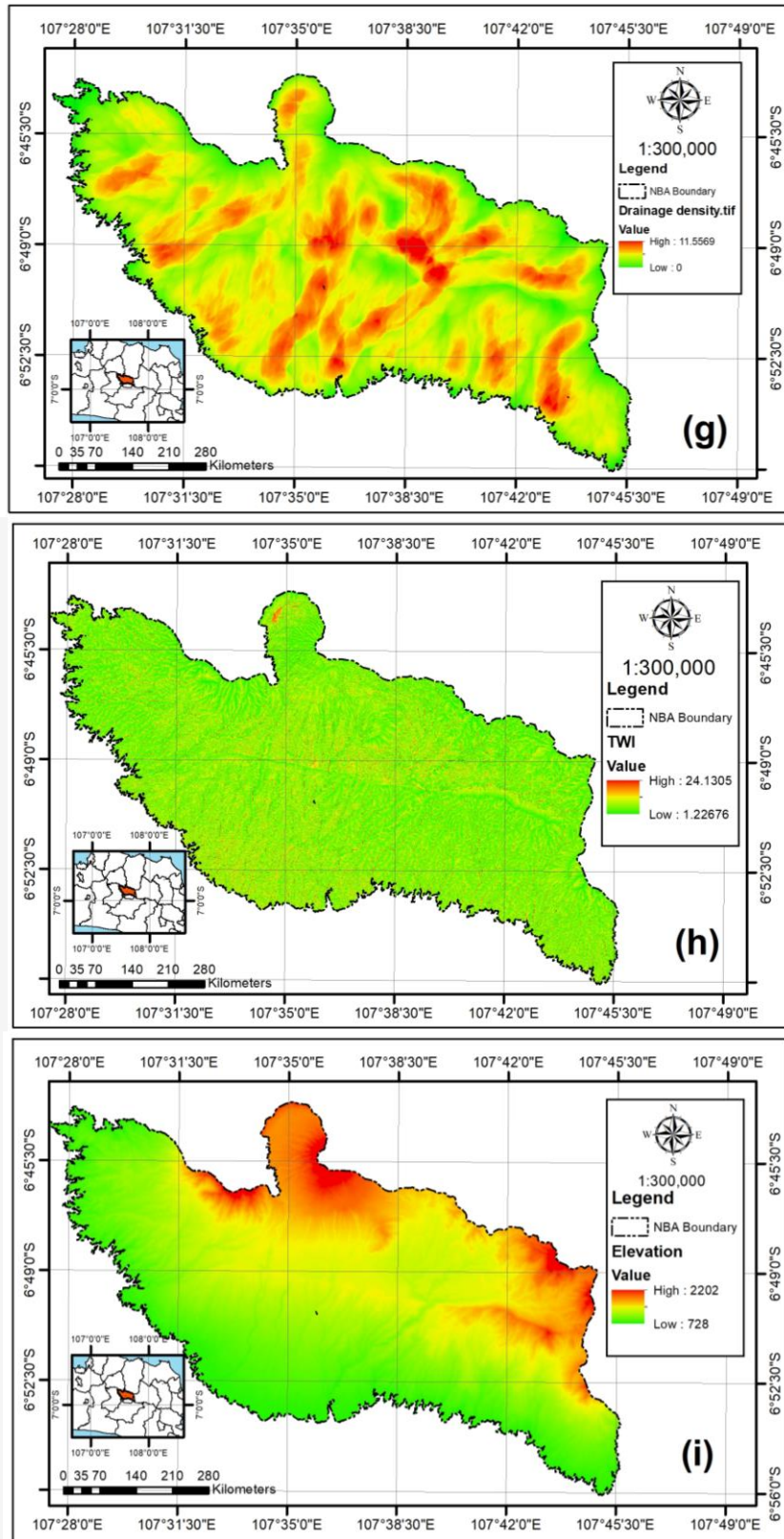


Figure 2: Variable landslide (g) Drainage distance, (h) TWI, (i) Elevation

4.2 Drainage Distance

Distance drainage in the study area has a maximum distance of 150m. Each classification is divided by 50m, so there are 3 classifications. Based on DEMNAS data extraction, the length of the river is 930.22 km. This condition is the accumulation of several river orders. Each area adjacent to 50m is an area that is easily eroded, due to gravity, and an area that provides a path for runoff to the river. In the northern part of the study, the average river is close to existing land uses, such as forests, plantations, fields, weeds, and dry fields. In the southern part, almost several locations are close to settlements, this condition is because in the southern part the topography is relatively low and the slope is not steep. In the western and eastern parts of the river are relatively close to the plantation area. Distance drainage can be seen in Figure 2.

4.3 Drainage Density

Drainage density values in the study area are 0 to 11.5569 km². The average river meeting area is on a fault line that stretches from east to west. In this area an active river is found which has several branches with natural formations. Several locations form river densities that follow or combine with fault lines. Based on the analysis, the densest area is in the middle of the study area where the river's water originates from the volcano, then flows through the structural area, and that's where it spreads naturally to form river orders. Of course, water will flow according to gravity, but the surrounding landforms will affect the flow pattern of the river. Tangkubanparahu has several springs which are the source of the river flow and flow into the Lembang fault area. Several locations have waterfalls indicating that the area is traversed by a Lembang fault. Drainage density can be seen in Figure 2.

4.4 Slope Angle

The slope angle study in the North Bandung area has a slope value of 0% - 165.072%. Figure 2 shows that the majority of steep slopes are in the northern area of the study, which is a volcanic landform, apart from that in the middle area there are structural faults that stretch from east to west, and almost every stretch has steep slopes. In the northern area there are two mountains with active and passive status. On the active volcano, Tangkuban Parahu, the slopes are steep, but in an indirect pattern, but slowly steeper towards a gentle slope. In the Burangrang passive mountain area, the slope of the slope is very steep, this condition occurs because Burangrang Mountain is an old mountain, so that erosion has occurred on the slopes since ancient times, this erosion has resulted in Burangrang Mountain having a very steep

average terrain. In the southern area of the study, the slope of the relatively sloping slopes decreases from the highlands in the north to the lowlands in the south.

4.5 Slope Aspect

The slope aspect in the study area has 10 types, namely flat (-1), North (0-22.5), Northeast (22.5-67.5), East (67.5-112.5), Southeast (112.5-157.5), South (157.5-202.5), Southwest (202.5-247.5), West (247.5-292.5), Northwest (292.5-337.5) and North (337.5-360), details can be seen in Figure 2. In the structural area, the average aspect slope faces North and Northeast. Overall, the slope aspect is quite varied, in the two landforms, both structural and volcanic, have different faces. In the baray, north and east the slopes tend to be southwest and west. That direction is the location of the sunset. The volcano area at the foot of the mountain to the north shows that the slope aspect is mostly facing East. In the southern area it tends to vary evenly, each slope has a variety of slope aspect types.

4.6 Distance Lineament

The lineament in this study is a form of alignment of the earth's surface in the North Bandung area. Based on the results of DEMNAS extraction, the total lineament length is 1,544.48 km with a total of 2,747 lineaments. Total distance lineament on each item is 150 m, with 3 classifications. The area near 50 m is a zone of brittle vulnerable material, because it tends to be near valleys that have high gravitational forces, and there are also pressures both internally and externally which cause this area to be exposed to erosion. The average existing zone near the lineament is forest, plantation, fields, dry fields and weeds. This condition concludes that the majority lineament is in the volcanic and structural landform area. In the southern area, lineament studies tend to be rare, because this area is already on a fairly gentle slope.

4.7 Elevation

Based on the pixel values at DEMNAS it was found that the elevation of the North Bandung area is 2202 masl to 728 masl. The highest area is in the volcanic landform, specifically Mount Tangkuban Parahu. Around the location of Mount Tangkuban Parahu, there is another plateau, namely Mount Burangrang. The zones around Tangkuban Parahu and Burangrang are highlands, so the pattern of land use in the surrounding area is typical of the highlands, such as the number of horticultural plantations. The lowest plains are in the southern area which is an urban area. The lowlands have entered a basin area called the Bandung basin. Specifically, the elevation of the North Bandung area can be seen in Figure 2.

4.8 Slope Curvature

In the study area there are all forms of slope curvature, namely concave, convex and straight. Based on the analysis of the slope curvature value, namely -31.5825 to 30.1469. In the concave condition the highest curvature value is -31.5825, while in the convex area the highest curvature value is 30.1469. This value is a general curvature value in volcano and structural landform. Volcanic and structural areas of course have varied slopes, in this section there is no dominance between concave, convex and straight, all of which have flat curvature characteristics. In the valley area it can be seen that the curvature forms convex, some are concave, the value of the curvature certainly influences the stability of the slopes in the volcano and structural landform area.

4.9 TWI (Topographic Wetness Index)

The condition of the Topographic wetness Index (TWI) value in the North Bandung area is 1.22676 to 24.1305. High TWI values in volcanic and structural landforms are in valley areas adjacent to rivers or lineaments. The TWI value is a value that functions for hydrological control with a damp indication. High TWI areas with steep topography can be indicators of erosion vulnerability. TWI in the entire area in the North Bandung Region has relatively no value dominance. The varied topography makes the TWI values spread evenly. Specifically, the distribution of TWI patterns can be seen in Figure 2.

4.10 Land Use Land Cover (LULC)

The results of the analysis show that there are 9 types of LULC in the North Bandung area. Land classification is adjusted to map scale which visualizes LULC information based on interpretation. LULC classifications are forest, orchard, rice field, field, built-up, water body, scrub, grassland, and rocky ground. The widest LLC type is dominated by a field of 11,865.26 ha, while the smallest area is rocky ground, which is 3.96 ha. North Bandung Kanan is a plateau with volcanic and structural landforms, this condition causes LULC in the North Bandung area to be dominated by fields. In this area there are many horticultural plants. The second dominance is the orchard type LULC. Clearer information regarding LULC is visualized in Figure 3.

4.11 Fuzzy Analysis of Landslide

Landslides in the North Bandung area are divided into three classes, namely high, medium and low. Based on the analysis of the area of each classification, namely high 36.27 km², medium 52.94

km², and low 11.77 km². The spatial distribution of high landslides is in the core area of the volcano and structural landform. The mountainous areas in the Tangkuban Parahu Mountains, Burangrang Mountains and the Lembang Fault are included in the landslide-prone zone. The specific location of the landslide is in the valley area adjacent to the river and lineament, so that it forms a pattern following these two variables. In the southern area, the majority are prone to landslides due to low land. Some parts that are not included in the classification are safe zones that are not potentially prone to landslides. More detailed information can be seen in Figure 4.

4.12 LULC Recommendations

Based on the results of the analysis of all types of LULC including areas prone to landslides in the classification of low, medium and high, except for the Rocky Ground LULC type. The rocky ground LULC type is a lifting area on the lembang fault line. This area has an area of 3.9 ha. The affected areas are built-up, field, forest, grassland, orchard, rice field, scrub, and water bodies which are presented in Figure 5. Based on the study the widest area affected by the high classification is the field, because it is located in a location that is generally on the edge ridge with steep slopes, and adjacent to the lineament and drainage. Built-up areas and several types of land are also included in the vulnerable zone, so a LULC recommendation is needed to anticipate landslide impacts.

The overlay map of the results of the landslide study and LULC found that there are several types of LULC that must be converted to land use to minimize landslides. In the high classification area, the land types that must be converted are rice fields (3,859,459.26 m) to orchards, built-up (992,895.23 m) to fields. In the medium classification, the land types that must be converted are rice fields (7,313,064.43 m) to orchards and built-ups (2,747,621.33 m) to fields. In the low classification area, the land types converted are orchards (27,658,447.99 m) to forest and rice fields (16,364,153.76 m) to orchards. In the classification of orchard type land conversion, trees such as palms, bamboo, kawung, and sugar palms can be planted, which essentially have small roots that grip the soil material and allow for high vegetation density. On land with a slope of 15%, it is better to make terracing and create annual crop schemes so that the land remains productive and minimizes landslides. Seasonal plants are not recommended, the recommended plants are plants with broad leaves, in order to prevent rain splashes before they reach the surface of the earth (Figure 5).

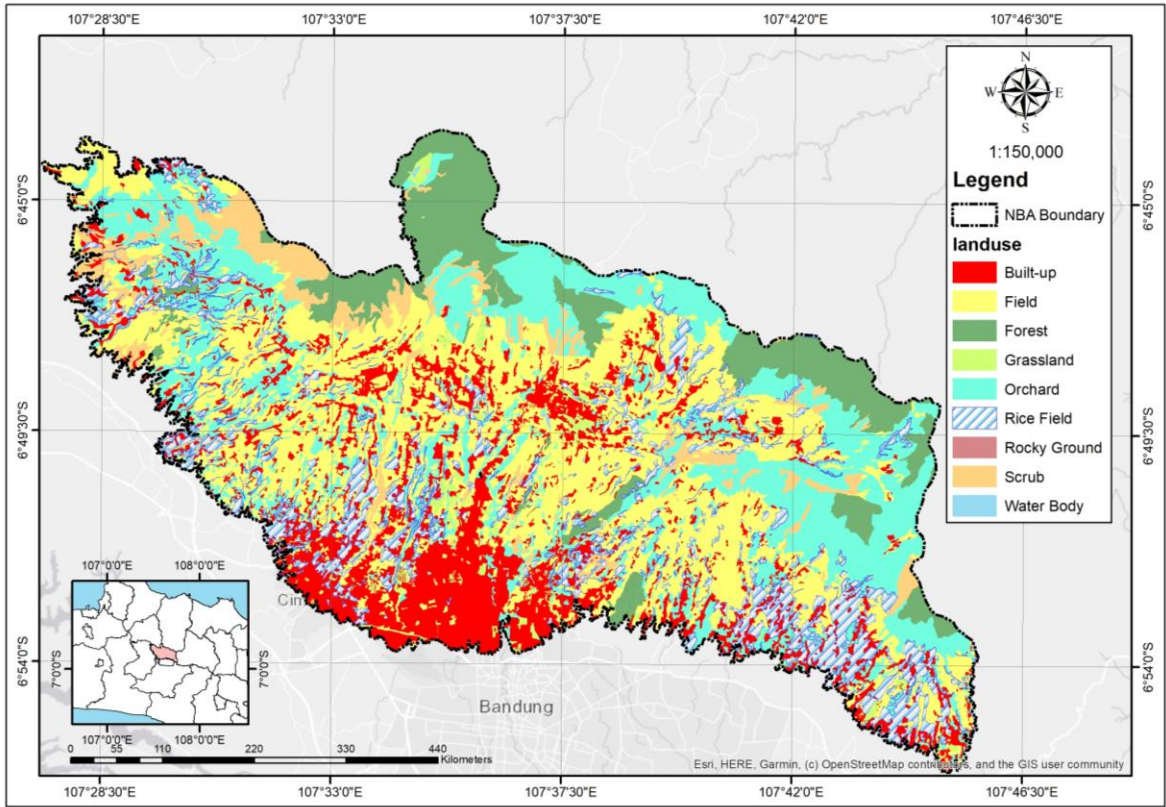


Figure 3: Land-Use/Land-Cover map of North Bandung area

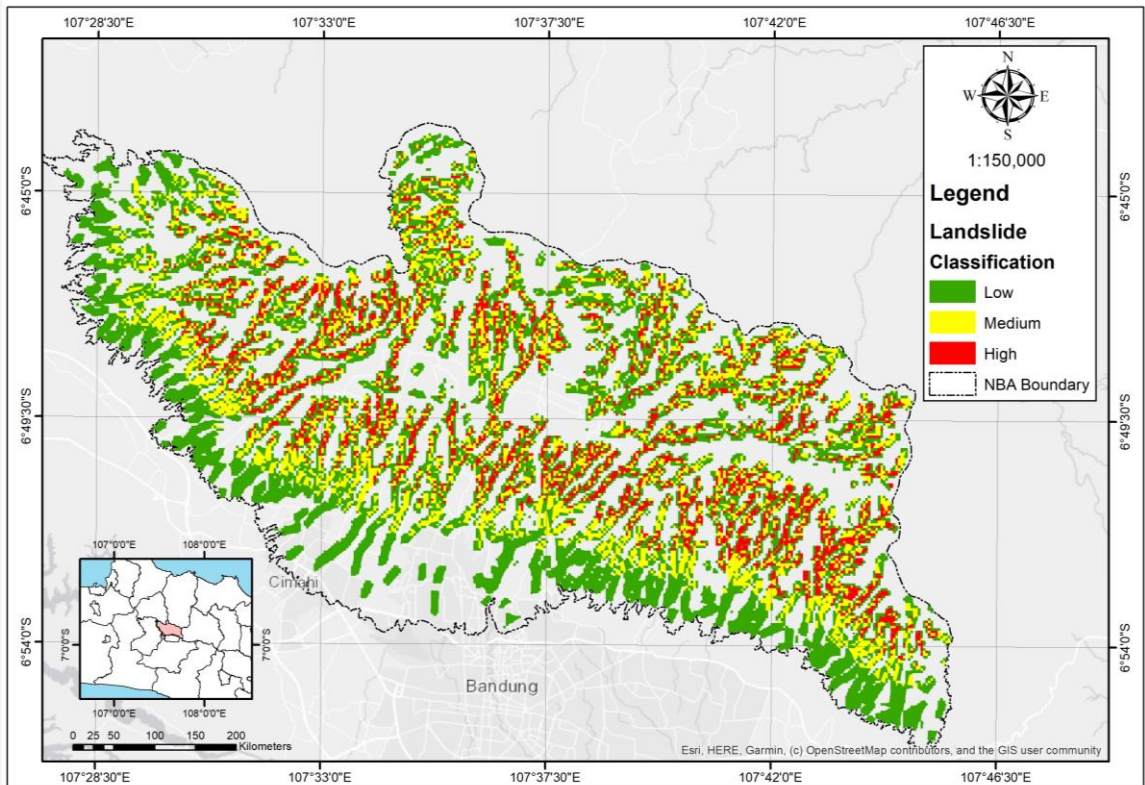
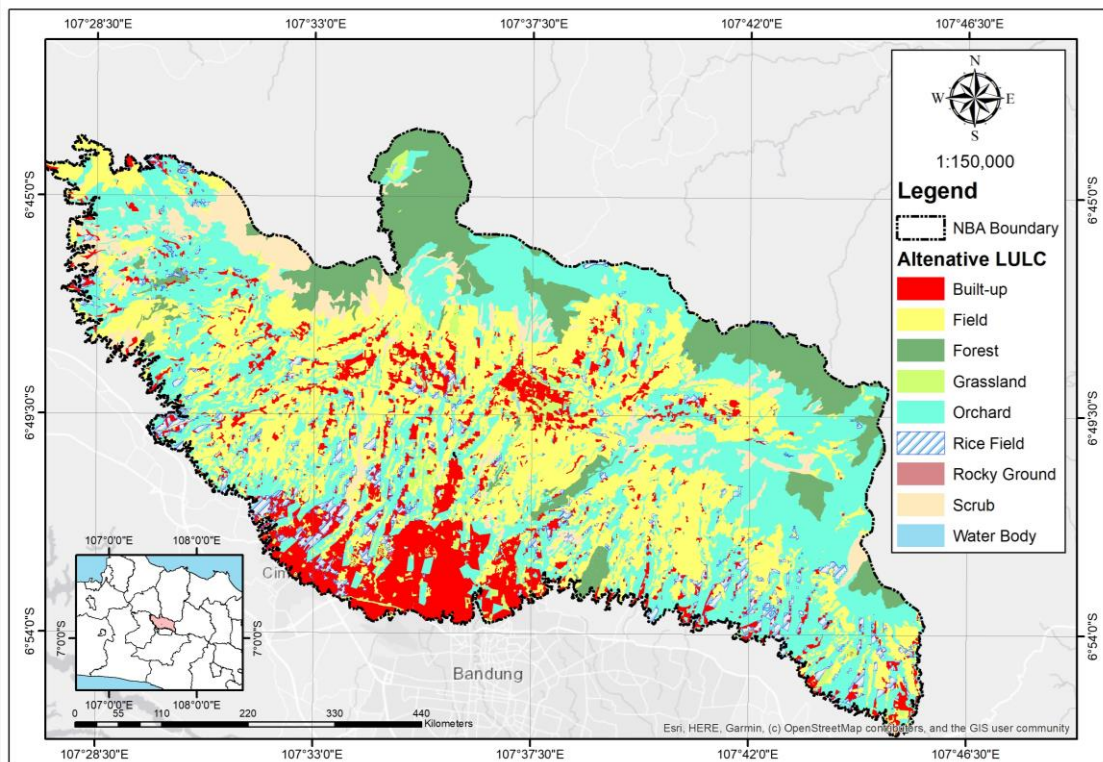


Figure 4: Landslide map of North Bandung area

Table 2: LULC area impacted by landslide

LULC	Landslide Classification Area (m ²)			LULC Total Area (m ²)
	Low	Medium	High	
Built-up	15,043,000.82	2,747,621.34	992,895.23	63,162,656.96
Field	35,021,349.88	17,807,628.50	14,084,502.33	118,652,589.2
Forest	9,400,064.14	6,151,207.56	3,393,322.34	41,177,835.1
Grassland	1,303,999.50	311,151.10	63,196.26	6,306,339.818
Orchard	27,658,448.01	14,378,845.78	10,687,365.69	92,978,115.02
Rice field	16,364,153.76	7,313,064.52	3,859,459.28	43,187,537.59
Rocky Ground	0	0	0	39,641.40625
Scrub	6,573,206.41	4,211,016.87	3,183,282.67	23,911,473.15
Water Body	55,420.21	8,196.36	4,232.31	194,000.0603
Total	111,769,173.28	52,945,344.51	36,269,792.83	389,610,188.31

**Figure 5:** Alternative Land-Use/Land-Cover map of North Bandung area

5. Conclusion

The North Bandung area includes volcanic and structural landform areas. This area contains active volcanoes and active faults, thus affecting slope stability. LULC in landslide-prone areas needs to get more attention, in order to minimize the risk of landslides. Based on the rain study in the North Bandung area, it is high. In general, the study area has tight drainage so that each line is almost close together. The slopes in the study area are way too steep, on the slope aspect there are 10 types and they

adjust to the cardinal directions. Slope curvature has a value of -31.5825 to 30.1469 with an elevation of 728 MSL to 2202 MSL. The lineament in the study area is 2,474 with a TWI value of 1.22676 to 24.1305. This condition requires the compatibility of landslide-prone to LULC. The analysis shows that there are 9 types of LULC, the widest type of LULC is dominated by a field of 11,865.26 ha, while the smallest area is rocky ground which is 3.96 ha. Based on the analysis of the area of each classification, namely high 36.27 km², medium 52.94 km², and low 11.77 km².

Based on the study of the widest area affected by the high classification, namely fields, because they are located in locations that are generally on the edge of a ridge with steep slopes, and are close to lineament and drainage. Built-up areas and several types of land are also included in the vulnerable zone, so a LULC recommendation is needed to anticipate landslide impacts. In the high classification area, the land types that must be converted are rice fields to orchards, built-ups to fields. In the medium classification, the land types that must be converted are rice fields to orchards and built-ups to fields. In the low classification area, the land types that are converted are orchards to forests and rice fields to orchards.

References

- [1] Asmare, D., (2022). Landslide Hazard Zonation and Evaluation around Debre Markos Town, NW Ethiopia: A GIS-based Bivariate Statistical Approach. *Scientific African*, Vol. 15. <https://doi.org/10.1016/j.sciaf.2022.e01129>.
- [2] Mekonnen, A. A., Raghuvanshi, T. K., Suryabhadgavan, K. V. and Kassawmar, T., (2022). GIS-based Landslide Susceptibility Zonation And Risk Assessment In Complex Landscape: A Case of Beshilo Watershed, Northern Ethiopia. *Environmental Challenges*, Vol. 8. <https://doi.org/10.1016/j.envc.2022.100586>.
- [3] Demir, G., (2019). GIS-Based Landslide Susceptibility Mapping for a Part of the North Anatolian Fault Zone between Reşadiye and Koyulhisar (Turkey). *Catena*, Vol. 183. <https://doi.org/10.1016/j.catena.2019.104211>.
- [4] Nicu, I. C., (2017). Frequency Ratio and GIS-based Evaluation of Landslide Susceptibility Applied to Cultural Heritage Assessment. *Journal of Cultural Heritage*, Vol. 28, 172–176. <https://doi.org/10.1016/j.culher.2017.06.002>.
- [5] Pham, B. T., Phong, T. Van, Nguyen-Thoi, T., Trinh, P. T., Tran, Q. C., Ho, L. S., Singh, S. K., Duyen, T. T. T., Nguyen, L. T., Le, H. Q., Le, H. Van, Hanh, N. T. B., Quoc, N. K. and Prakash, I., (2020). GIS-Based Ensemble Soft Computing Models for Landslide Susceptibility Mapping. *Advances in Space Research*, Vol. 66(6), 1303–1320. <https://doi.org/10.1016/j.asr.2020.05.016>.
- [6] Bragagnolo, L., da Silva, R. V. and Grzybowski, J. M. V., (2020). Landslide Susceptibility Mapping with r.landslide: A Free Open-Source GIS-Integrated Tool Based on Artificial Neural Networks. *Environmental Modelling and Software*, Vol. 123. <https://doi.org/10.1016/j.envsoft.2019.104565>.
- [7] Ali, S. A., Parvin, F., Vojteková, J., Costache, R., Linh, N. T. T., Pham, Q. B., Vojtek, M., Gigović, L., Ahmad, A. and Ghorbani, M. A., (2021). GIS-Based Landslide Susceptibility Modeling: A Comparison between Fuzzy Multi-Criteria and Machine Learning Algorithms. *Geoscience Frontiers*, Vol. 12(2), 857–876. <https://doi.org/10.1016/j.gsf.2020.09.004>.
- [8] Raghuvanshi, T. K., Negassa, L. and Kala, P. M., (2015). GIS based Grid overlay method versus modeling approach - A comparative study for landslide hazard zonation (LHZ) in Meta Robi District of West Showa Zone in Ethiopia. *Egyptian Journal of Remote Sensing and Space Science*, Vol. 18(2), 235–250. <https://doi.org/10.1016/j.ejrs.2015.08.001>.
- [9] Abbas, N., Afsar, S., Jan, B., Sayla, E. A. and Nawaz, F., (2022). GIS Based Model for the Landslides Risk Assessment. A Case Study in Hunza-Nagar Settlements, Gilgit-Baltistan, Pakistan. *Environmental Challenges*, Vol. 7. <https://doi.org/10.1016/j.envc.2022.100487>.
- [10] Chen, X. and Chen, W. (2021). GIS-based Landslide Susceptibility Assessment Using Optimized Hybrid Machine Learning Methods. *Catena*, Vol. 196. <https://doi.org/10.1016/j.catena.2020.104833>.
- [11] Chen, W. and Zhang, S., (2021). GIS-Based Comparative Study of Bayes Network, Hoeffding Tree and Logistic Model Tree for Landslide Susceptibility Modeling. *Catena*, Vol. 203. <https://doi.org/10.1016/j.catena.2021.105344>.
- [12] Berhane, G., Kebede, M., Alfarah, N., Hagos, E., Grum, B., Giday, A. and Abera, T., (2020). Landslide Susceptibility Zonation Mapping Using GIS-based Frequency Ratio Model with Multi-Class Spatial Data-Sets in the Adwa-Adigrat Mountain Chains, Northern Ethiopia. *Journal of African Earth Sciences*, Vol. 164. <https://doi.org/10.1016/j.jafrearsci.2020.103795>.
- [13] Basu, T. and Pal, S., (2019). RS-GIS Based Morphometrical and Geological Multi-Criteria Approach to the Landslide Susceptibility Mapping in Gish River Basin, West Bengal, India. *Advances in Space Research*, Vol. 63(3), 1253–1269. <https://doi.org/10.1016/j.asr.2018.10.033>.

- [14] Jiao, Y., Zhao, D., Ding, Y., Liu, Y., Xu, Q., Qiu, Y., Liu, C., Liu, Z., Zha, Z. and Li, R., (2019). Performance Evaluation for four GIS-based Models Purposed to Predict and Map Landslide Susceptibility: A Case Study at a World Heritage Site in Southwest China. *Catena*, Vol. 183. <https://doi.org/10.1016/j.catena.2019.104221>.
- [15] Gutiérrez-Martín, A., (2020). A GIS-Physically-Based Emergency Methodology for Predicting Rainfall-Induced Shallow Landslide Zonation. *Geomorphology*, Vol. 359. <https://doi.org/10.1016/j.geomorph.2020.107121>.
- [16] Shu, H., Hürlimann, M., Molowny-Horas, R., González, M., Pinyol, J., Abancó, C. and Ma, J., (2019). Relation between Land Cover and Landslide Susceptibility in Val d'Aran, Pyrenees (Spain): Historical Aspects, Present Situation and Forward Prediction. *Science of the Total Environment*, Vol. 693, 1–14. <https://doi.org/10.1016/j.scitotenv.2019.07.363>
- [17] Alsabhan, A. H., Singh, K., Sharma, A., Alam, S., Pandey, D. D., Rahman, S. A. S., Khursheed, A. and Munshi, F. M., (2022). Landslide Susceptibility Assessment in the Himalayan Range Based along Kasauli – Parwanoo Road Corridor Using Weight of Evidence, Information Value, and Frequency Ratio. *Journal of King Saud University - Science*, Vol. 34(2). <https://doi.org/10.1016/j.jksus.2021.101759>.
- [18] Sonker, I., Tripathi, J. N. and Singh, A. K., (2021). Landslide Susceptibility Zonation Using Geospatial Technique and Analytical Hierarchy Process in Sikkim Himalaya. *Quaternary Science Advances*, Vol. 4. <https://doi.org/10.1016/j.qsa.2021.100039>.
- [19] Gadrani, L., Lominadze, G. and Tsitsagi, M., (2018). F assessment of Landuse/Landcover (LULC) change of Tbilisi and Surrounding Area Using Remote Sensing (RS) and GIS. *Annals of Agrarian Science*, Vol. 16(2), 163–169. <https://doi.org/10.1016/j.aasci.2018.02.005>.
- [20] Guo, Z., Torra, O., Hürlimann, M., Abancó, C. and Medina, V., (2022). FSLAM: A QGIS Plugin for Fast Regional Susceptibility Assessment of Rainfall-Induced Landslides. *Environmental Modelling and Software*, Vol. 150. <https://doi.org/10.1016/j.envsoft.2022.105354>.
- [21] Tiwari, S., Kumar Jha, S. and Sivakumar, B., (2019). Reconstruction of Daily Rainfall Data Using the Concepts of Networks: Accounting for Spatial Connections in Neighborhood Selection. *Journal of Hydrology*, Vol. 579. <https://doi.org/10.1016/j.jhydrol.2019.124185>.
- [22] Bassey Eze, E. and Efiog, J., (2010). Morphometric Parameters of the Calabar River Basin: Implication for Hydrologic Processes. *Journal of Geography and Geology*, Vol. 2(1). <https://doi.org/10.5539/jgg.v2n1p18>.
- [23] Chen, W. and Li, Y. (2020). GIS-based Evaluation of Landslide Susceptibility Using Hybrid Computational Intelligence Models. *Catena*, Vol. 195. <https://doi.org/10.1016/j.catena.2020.104777>.
- [24] Tan, Q., Bai, M., Zhou, P., Hu, J. and Qin, X., (2021). Geological Hazard Risk Assessment of Line Landslide Based on Remotely Sensed Data and GIS. *Measurement: Journal of the International Measurement Confederation*, Vol. 169. <https://doi.org/10.1016/j.measurement.2020.108370>.
- [25] Capitani, M., Ribolini, A. and Bini, M., (2013). The Slope Aspect: A Predisposing Factor for Landsliding? *Comptes Rendus - Geoscience*, Vol. 345(11–12), 427–438. <https://doi.org/10.1016/j.crte.2013.11.002>.
- [26] Du, F., Okazaki, K., Ochiai, C. and Kobayashi, H., (2016). Post-Disaster Building Repair and Retrofit in a Disaster-Prone Historical Village in China: A Case Study in Shangli, Sichuan. *International Journal of Disaster Risk Reduction*, Vol. 16, 142–157. <https://doi.org/10.1016/j.ijdr.2016.02.007>.
- [27] Neuhäuser, B., Damm, B. and Terhorst, B., (2012). GIS-Based Assessment of Landslide Susceptibility on the Base of the Weights-of-Evidence Model. *Landslides*, Vol. 9(4), 511–528. <https://doi.org/10.1007/s10346-011-0305-5>.
- [28] Hammad Khaliq, A., Basharat, M., Talha Riaz, M., Tayyib Riaz, M., Wani, S., Al-Ansari, N., Ba Le, L. and Thi Thuy Linh, N., (2022). Spatiotemporal Landslide Susceptibility Mapping Using Machine Learning Models: A Case Study from District Hattian Bala, NW Himalaya, Pakistan. *Ain Shams Engineering Journal*, Vol. 14(3). <https://doi.org/10.1016/j.asej.2022.101907>.
- [29] Panchal, S. and Shrivastava, A. K., (2022). Landslide Hazard Assessment Using Analytic Hierarchy Process (AHP): A Case Study of National Highway 5 in India. *Ain Shams Engineering Journal*, Vol. 13(3), 101626. <https://doi.org/10.1016/j.asej.2021.10.021>.

- [30] Hargono, B., Sartohadi, J., Pramonohadi, M. and Setiawan, B., (2014). Spatial Model for Ground Water Conservation Based on Landform Approach in the Southern Flank of Merapi Vulcano. *Journal of Geography and Earth Sciences*, Vol. 2(2), 1–20. <https://doi.org/10.15640/jges.v2n2a1>.
- [31] Ihsan, H, M., Hadi, M, P. and Sartohadi, J., (2020). Step-wise Overlay Technique for the Mapping of Unconfined Groundwater Potential Zone in Tectonically Controlled Landforms. *International Journal of Geoinformatics*, Vol. 16, 20–28. <https://journals.sfu.ca/ijg/index.php/journal/article/view/1791>.
- [32] Hao, L., van Westen, C., Rajaneesh, A., Sajinkumar, K. S., Martha, T. R. and Jaiswal, P., (2022). Evaluating the Relation between Land Use changes and the 2018 Landslide Disaster in Kerala, India. *Catena*, Vol. 216(PA). <https://doi.org/10.1016/j.catena.2022.106363>.
- [33] Liao, M., Wen, H. and Yang, L., (2022). Identifying the Essential Conditioning Factors of Landslide Susceptibility Models Under Different Grid Resolutions Using Hybrid Machine Learning: A Case of Wushan and Wuxi Counties, China. *Catena*, Vol. 217. <https://doi.org/10.1016/j.catena.2022.106428>.